Acta Biotheoretica (2022) 70:23
https://doi.org/10.1007/s10441-022-09447-1

REGULAR ARTICLE

COVID-19 Adaptive Humoral Immunity Models: Weakly Neutralizing Versus Antibody-Disease Enhancement Scenarios

Antoine Danchin[1] · Oriane Pagani-Azizi[2] · Gabriel Turinici[3] · Ghozlane Yahiaoui[4]

Received: 14 January 2021 / Accepted: 23 June 2022 / Published online: 13 August 2022
© Prof. Dr. Jan van der Hoeven stichting voor theoretische biologie 2022

Abstract
The interplay between the virus, infected cells and immune responses to SARS-CoV-2 is still under debate. By extending the basic model of viral dynamics, we propose here a formal approach to describe neutralisation versus weak (or non-)neutralisation scenarios and compare them with the possible effects of antibody-dependent enhancement (ADE). The theoretical model is consistent with the data available in the literature; we show that both weakly neutralising antibodies and ADE can result in final viral clearance or disease progression, but that the immunodynamics are different in each case. As a significant proportion of the world's population is already naturally immune or vaccinated, we also discuss the implications for secondary infections after vaccination or in the presence of immune system dysfunctions.

Keywords Virus model · Virus - immune system interaction · Antibody disease enhancement · COVID-19 · SARS-CoV-2 · Non-neutralizing antibodies

✉ Gabriel Turinici
Gabriel.Turinici@dauphine.fr

Antoine Danchin
Antoine.Danchin@normalesup.org

Oriane Pagani-Azizi
Oriane.Pagani-Azizi@espci.fr

Ghozlane Yahiaoui
Ghozlane.Yahiaoui@maths.ox.ac.uk

1 School of Biomedical Sciences, University of Hong Kong, Hong Kong, China, 21 Sassoon Road, Pokfulam, 999077

2 CEREMADE - ESPCI Paris PSL, Paris, France

3 CEREMADE, Université Paris Dauphine - PSL Research University, Paris, France

4 Mathematical Institute, University of Oxford, Oxford, UK

1 Background

SARS-CoV-2 is a new virus of the coronavirus family, responsible for the ongoing COVID-19 pandemic. To date, there are more than 300 million cases and over five million deaths worldwide (John's Hopkins University 2000). SARS-CoV-2 is the third severe beta-coronavirus to emerge in the last 20 years, after SARS-CoV-1 and MERS-CoV. Hence the growing need for effective drugs and/or vaccines, not only in the immediate future but also in anticipation of a subsequent coronavirus resurgence.

However, the promising initial successes of antiviral treatments have also raised the possibility of negative side-effects. With regard to vaccines, an autoimmune disease (which lead to the temporary suspension of clinical trials) occurred during the AstraZeneca vaccine trial (9 September 2020); this context has demonstrated the importance of understanding qualitatively and quantitatively the immune response to primary infection and challenges (vaccines fall into both categories). In particular, relevant mathematical models of immune dynamics may be of interest to understand and predict the complicated behavior often observed.

We focus here on humoral adaptive immunity (antibody-mediated immunity) and refer to future works for an extension to the cellular and/or innate immune system. For clinical reasons and also for the understanding of those studying vaccines, antibody responses are of paramount importance. However, the neutralizing abilities of antibodies are still under discussion, especially as weak or non-neutralizing antibodies can promote infection through a process called antibody-dependent enhancement (hereafter abbreviated 'ADE') (Taylor et al. 2015; Iwasaki and Yang 2020; Yip et al. 2014; Jaume et al. 2011), see also the online supplementary information (Danchin et al. 2020). Therefore, here we studied both primary and secondary COVID-19.

To summarize, we propose a mathematical model of the immune response and virus dynamics that includes the possibility of weakly neutralizing antibodies and / or ADE and discuss its implications. At the time of writing the second version of the manuscript (January 2022) a significant part of the world's population is either vaccinated or naturally immunized and the consequences of reinfection events are a major source of uncertainty concerning the evolution of the pandemic. This situation naturally calls for scientific investigation.

2 Methods

2.1 Mathematical Model

We present below the viral and immune response model. It is a compartmental model similar to those used to describe the epidemic propagation, see Kermack and McKendrick (1927), Diekmann et al. (2000), Hethcote (2000), Ng et al. (2003) for a general introduction and Faraz et al. (2020), Drożdżal et al. (2021),

Liu et al. (2020), Danchin and Turinici (2021), Dolbeault and Turinici (2020) and Danchin et al. (2021) for COVID-19 specific works.

The viral-host interaction (excluding the immune response) is called the basic model of virus dynamics. It has been extensively validated both theoretically and experimentally, see Nowak and May (2000, Eq. (3.1), p. 18) and Wodarz (2007, Eqs. (2.3)–(2.4), p. 26) and references therein. See also Louzoun (2007), Castro et al. (2016) and Eftimie et al. (2016) for general overviews of mathematical immunology.

The model involves several classes: that of the target cells, denoted T, the infected cells, denoted I, the free virus denoted V and the antibodies denoted A. The model is illustrated in Fig. 1.

Target cells T, which in our case are the epithelial cells with ACE2 receptors located, for instance in the respiratory tracts including lungs, nasal and trachea/bronchial tissues, are produced at a rate Λ and die at rate μ. The parameters Λ and μ define tissue dynamics in the absence of infection, see also "Model Without a Virus, Nor Immune Response" section in "Appendix 3". When these susceptible cells meet free virus particles V, they become infected at a rate β_0. Furthermore, target cells can also become infected via ADE if virus entry is mediated by antibodies. The parameter β_1 represents the rate of ADE infection route which is the result of a three-species interaction: T, A and V.

Infected (initially target) cells, denoted I, die at a rate δ. Note that this death rate will often be larger than the death rate of uninfected cells because viruses cause cell damage and cell death, Wodarz (2007) and Nowak and May (2000). Infected cells produce new virus particles at a rate ω, and the free virus particles which have been released from infected cells decay at a rate c called the clearance rate.

Free virions are neutralized by antibodies A, which can block virus entry into cells but also facilitate phagocytosis, at a rate b. Finally, the antibodies can be stimulated by the free virus with a production rate a while declining at a rate of σ (see for instance Wodarz 2007, eq. (9.4), p.126)). Note that alternative proposals for

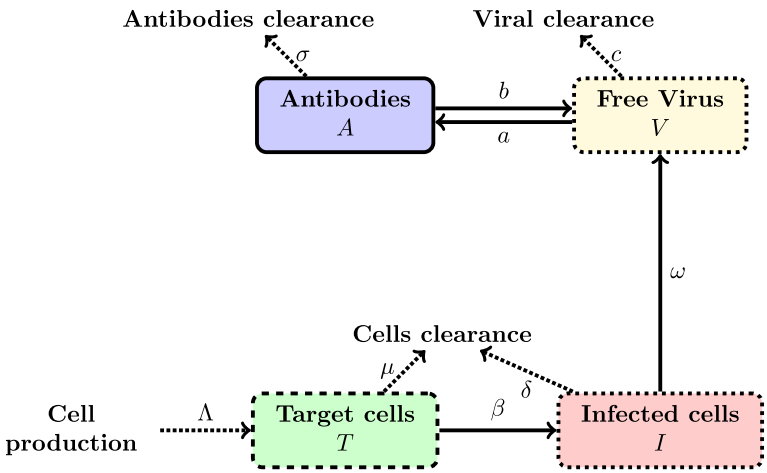

Fig. 1 Graphical illustration of the flow in the model (1)–(5)

the antibody dynamics exist, see e.g. André and Gandon André et al. (2006) who assume that immune response, once started, grows at a constant rate while Pawlek et al. (2016) design a more complex model that takes into account the macrophage activation. The complete model reads (all constants are positive):

$$dT/dt = \Lambda - \mu T - \beta(A)VT \tag{1}$$

$$dI/dt = \beta(A)VT - \delta I \tag{2}$$

$$dV/dt = \omega I - cV - bAV \tag{3}$$

$$dA/dt = aVA - \sigma A \tag{4}$$

$$\beta(A) = \beta_0 + \beta_1 A. \tag{5}$$

Several hypotheses in this model need to be further documented. The first one in that all infected cells including ADE infected cells support viral replication and can produce virus. However, to date, it is still unclear whether ADE infected cells can support viral replication in vivo, Yip et al. (2014) and Jaume et al. (2011). Here we choose not to distinguish between virus productive and non productive infected cells to keep the model simple (see however the comments in "Appendix 4"). For the same reason, we do not discriminate between neutralizing, weakly neutralizing or non-neutralizing antibodies but consider all as members of the same class, the antibodies neutralizing capacity will therefore be the average of the neutralizing power and the average is described by the parameter b; on the other hand the ADE magnitude will be monitored by parameter β_1. These parameters are the most important part of the immune response and the object of our study.

3 Stability of Equilibria and Further Considerations

We operate under the assumptions that all parameters are positive and furthermore the following two assumptions hold (see "Appendix 3" for details):

$$\text{Assumption 1:} \quad \delta > \mu. \tag{6}$$

$$\text{Assumption 2:} \quad \left(R_0 - 1\right)\frac{\mu}{\beta_0} > \frac{\sigma}{a}. \tag{7}$$

where we define as in Nowak and May (2000, Eq. (6.2), p. 53):

$$R_0 = \frac{\beta_0 \omega \Lambda}{c\delta\mu}. \tag{8}$$

Note that (7) implies in particular $R_0 > 1$ which is a standard condition for such models. We will further denote

$$V^{is} := \left(R_0 - 1\right)\frac{\mu}{\beta_0},\ V^t := \sigma/a. \tag{9}$$

3.1 Stability of the Equilibrium without ADE

With these definitions we can give the main theoretical properties of the model depending on the presence or not of the ADE term.

Proposition 1 *The model* (1)–(4) *without ADE i.e.*, $\beta(A) = \beta_0$ (*that is* $\beta_1 = 0$) *has a single stable equilibrium given by*:

$$T = \frac{\Lambda}{\mu + \beta_0 V^t},\ I = \frac{\beta_0 \Lambda V^t}{\delta(\mu + \beta_0 V^t)},\ V = V^t,\ A = \frac{c(V^{is} - V^t)}{\beta_0 b(\mu + \beta_0 V^t)}. \tag{10}$$

Proof The proof of the stability of the equilibrium (10) is technical and is given in full detail in "Model: Virus and Immune Response but No Enhancement" section in "Appendix 3". □

3.2 Stability of the Equilibrium with ADE

We investigate now the full model having a non-null ADE term $\beta_1 > 0$.

Proposition 2 *The model* (1)–(4) *has three equilibria*:

1. *the trivial equilibrium* $T = T^* = \Lambda/\mu, V = I = A = 0$ *which is unstable*;
2. *the immmunosuppression equilibrium*, *also unstable*, *given by* :

$$T = T^{is} := \frac{\delta c}{\beta_0 \omega},\ I = I^{is} := \left(R_0 - 1\right)\frac{c\mu}{\omega\beta_0},\ V = V^{is} := \left(R_0 - 1\right)\frac{\mu}{\beta_0},\ A = 0. \tag{11}$$

3. *and a third equilibrium characterized as follows*:
   - the antibody level A^f is the unique positive solution of the following second order equation in the unknown A:

$$\omega\beta(A)\Lambda = \delta(c + bA)(\mu + \beta(A)V^t); \tag{12}$$

   - the other quantities are:

$$T^f = \frac{\delta(c + bA^f)}{\omega\beta(A^f)},\ I^f = \frac{V(c + bA^f)}{\omega},\ V = V^t = \frac{\sigma}{a}. \tag{13}$$

The following affirmations hold true concerning this third equilibrium

(a) when β_1 is small enough the equilibrium is stable;

(b) when β_1 is large enough the equilibrium is stable;
(c) however there exist choices of parameters (in particular values of β_1) for which this equilibrium is unstable.

Proof The proof is presented in "Appendix 3".

3.3 Dynamical Aspects

The equilibrium analysis in the previous sections does not yet tell the full story of the evolution of the system (1)–(4). Depending on the parameters, a common behavior is the following: initially A will increase as response to V being above threshold V^t; the increase of A will drive both I and V to zero. Such a dynamics is stable over a long period and in practice I and V will keep small values for a time long enough to ensure virus clearance (when V is small enough, due to the random nature of the events, V will disappear).

Taking I and V to be constant equal to zero, the new evolution is:

$$dT/dt = \Lambda - \mu T \tag{14}$$

$$dA/dt = -\sigma A. \tag{15}$$

Note that equations for I and V are missing because if the initial states are $V(0) = I(0) = 0$ then $V(t) = I(t)$ for all $t \geq 0$. This evolution drives T to Λ/μ and A to zero. If however during the slow decay of A a challenge is presented in the form of a virus load $V > \sigma/a$ a new infection will start and V and I will rise again.

In conclusion, the stable equilibrium (12)–(13) is not necessarily reached in practice. The precise dynamics depends crucially on the parameters b and β_1, see main text for details.

4 Results

4.1 Theoretical Results

We refer the reader to Sect. 3 for the rigorous statements concerning the theoretical properties of the model (1)–(5). Several situations may occur, but in summary the absence of ADE (i.e., $\beta_1 = 0$) insures stable equilibrium while intermediate β_1 values (neither too small not too large) may provide examples of unstable equilibria; moreover, stochastic events prevent the stable equilibrium state to be reached in practice, cf. Sect. 3.3. The parameters b and β_1 are shown to be the most important for the viral-host-antibody dynamics.

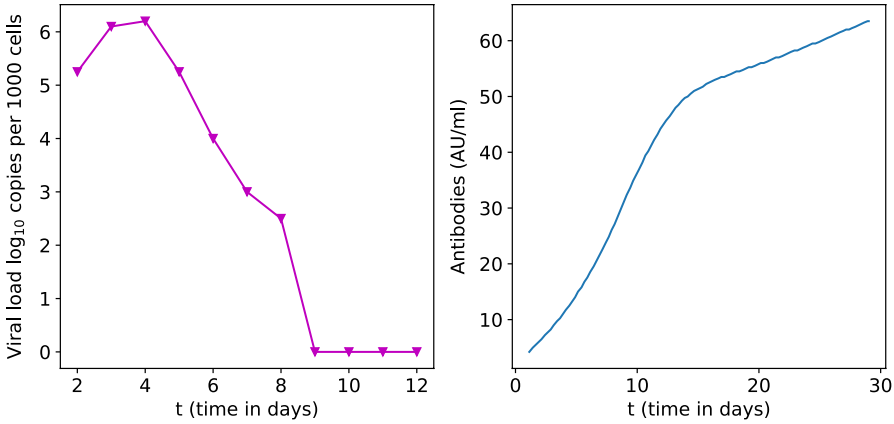

Fig. 2 *Left* Clinically observed typical variation of SARS-CoV-2 viral load in nasopharyngeal swab normalised using cell quantification. Data taken from Lescure et al. (2020, Fig. 3, p. 703, patient 4). *Right* Typical time variations for IgG. Data taken from Padoan et al. (2020, Fig. 2, p. 1085). Note that the antibody data is a mean over several days and corresponds to a different patient cohort

Table 1 Baseline parameters use in numerical simulations of the model (1)–(4)

μ	Λ	ω	β_0	β_1	δ	c	b
9.66	9.66×10^6	59.74	1.28×10^{-6}	0	16.22	1.45	0.52
a	σ	$I(0)$	$V(0)$	$A(0)$			
9.15×10^{-7}	0.02	372.11	994.84	1.17			

4.2 Empirical Results: Initial Infection

Taking into account the available data from the literature and the methodology in "Appendix 1" we run a numerical procedure to fit the model parameters to reproduce at best the viral load data in Fig. 2 (left) and obtained the values in Table 1. The numerical simulation for a primary infection corresponding to these parameters is shown in Fig. 3.

There is a 20% fall of target cells which either become infected or naturally die. The viral load peaks around 4-5 days after symptoms onset at 1.8×10^6 copies/ml. While SARS-CoV-1 viral load, as MERS-CoV, peaked around 10 days after symptoms onset, most studies agree that SARS-CoV-2 viral load peaks sooner, around 5 days, Lescure et al. (2020) and Zou et al. (2020). Concerning antibodies, they increase sharply until week 2 then slower until a month after infection and start to decrease within 2–3 months (Long et al. 2020; Seow et al. 2020). Qualitative agreement is observed with clinically observed variations variations of viral load and partially with antibodies concentration depicted in Fig. 2 (see references in the figure).

Note that, although we expect agreement between $V(t)$ and the viral load evolution in Fig. 2 (left) (which corresponds to a precise, real patient) the antibody

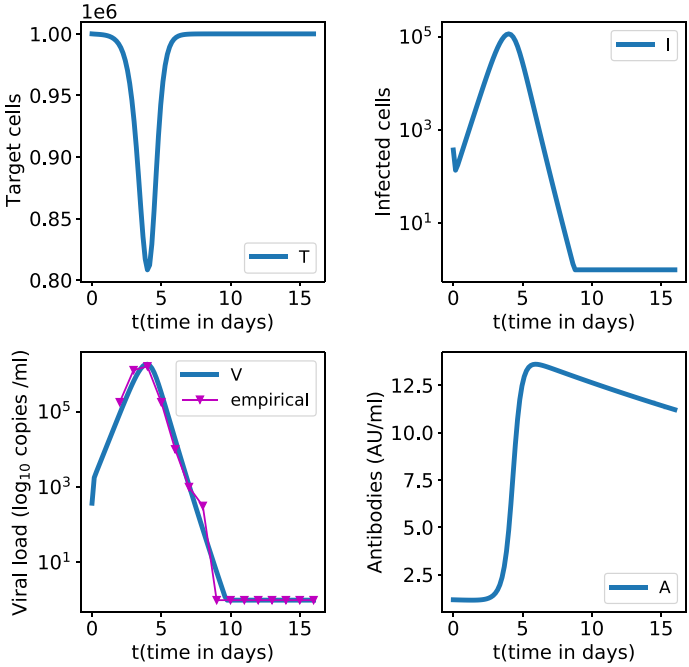

Fig. 3 Numerical simulation of the first infection without ADE for model (1)–(4) and parameters in Table 1. A good fit for the viral load from Fig. 2 is obtained (data is truncated below the value 1). On the contrary the fit is not as good for $A(t)$ because data does not correspond to the same patient (joint $V(t)/A(t)$ data was not available)

data from Padoan et al. (2020, Fig. 2, p. 1085) does not correspond to the same patient (data unavailable) but is a mean value over several days and patients (not always the same). Each individual is likely to have his own immuno-kinetic parameters: the parameters of the individual that may fit the $A(t)$ data from Fig. 2 (right) are not the same as the parameters that fit the data in left side of the same figure.

The equilibrium state (10) when $\beta_1 = 0$ (no ADE present) is reached after 2 years for all variables in Fig. 3. However, viral load and infected cells reach a minimum within several weeks post-infection before increasing and oscillating toward equilibrium state (10) (simulations not shown here). Therefore, if the virus load is very small close to the minimum, all other variables decrease towards 0 and the infection has vanished. The equilibrium state (10) is stable but not reached in practice as the patient is cured.

4.3 Empirical Results: Secondary Infection, Variants, Vaccination

We focus on a scenario where the immuno-kinetic parameters such as the neutralizing efficacy (b) or the ADE parameter (β_1) change; the causes can be multiple: a primary infection with a different variant, vaccination, or some immune evolution

(aging being an example). In all cases we investigate the infection, called challenge, that takes place with a different set of b of β_1 parameters than in Table 1.

4.3.1 Variation of the Neutralizing Capacity *b*

When there is no ADE, decreasing the neutralizing capacity of antibodies (parameter b) leads on the one hand to a higher viral load peak but on the other hand to higher antibodies concentrations. The less neutralizing the antibodies are, the more abundant they are in order to have the infection always cleared. The simulations results are presented in Fig. 4. Infection resolution is obtained with little target cell destruction for larger values of b. On the contrary, low values of b will lead to significant increase of the antibody number and simultaneous decay of target cells, both largely pejorative for the patient.

In the cases where the viral load reaches low values the infection stops before converging to the theoretical equilibrium.

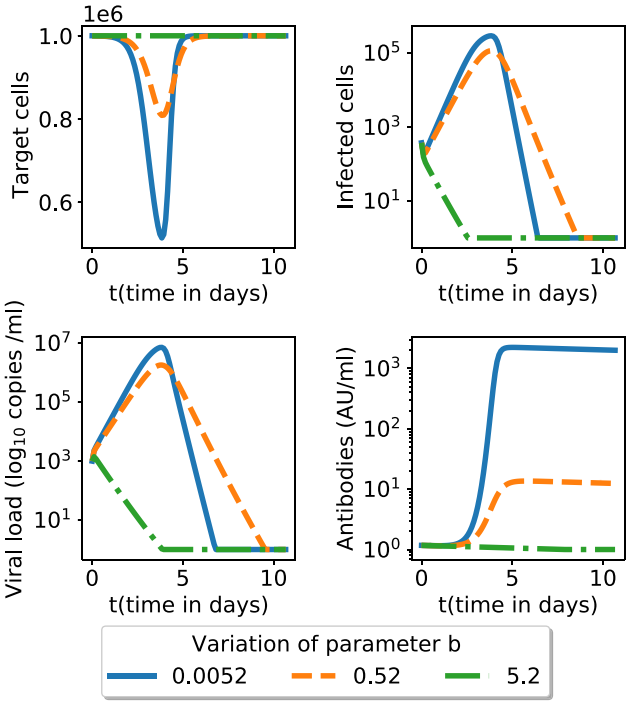

Fig. 4 Numerical simulation of the model (1)–(4) and parameters in Table 1. Only the neutralizing capacity b is changed around the nominal value $b = 0.52$. Lower value of the neutralizing capacity b (solid blue line) leads to lower target cell count and higher antibody levels. See Fig. 6 for simulation over a longer time span

4.3.2 Presence of ADE ($\beta_1 > 0$)

We investigated in Figs. 5 and 6 the possibility of the ADE mechanism present ($\beta_1 > 0$), for a range of possible parameter β_1 values. We plot all variables upon challenge with the same neutralizing capacity for antibodies. A higher ADE parameter leads to more destroyed target cells, more infected cells, more viral load and more antibodies. However the antibodies concentration is restricted by an upper limit (see Fig. 5 and compare with theoretical insights in the proof of point 3b of Proposition 2 in "Appendix 3"). Therefore after some threshold value, a higher β_1 ADE parameter cannot be compensated by more antibodies.

For example, unlike $\beta_1 = 10^{-8}$, if $\beta_1 = 10^{-6}$ the viral load directly stabilizes to its equilibrium state (13), without reaching a minimum close to 0 while oscillating (simulation not shown here). In this case, the infection wins (leading to respiratory function disruption and possibly patient death). Large values of β_1 lead to significant (possibly total) destruction of target cells.

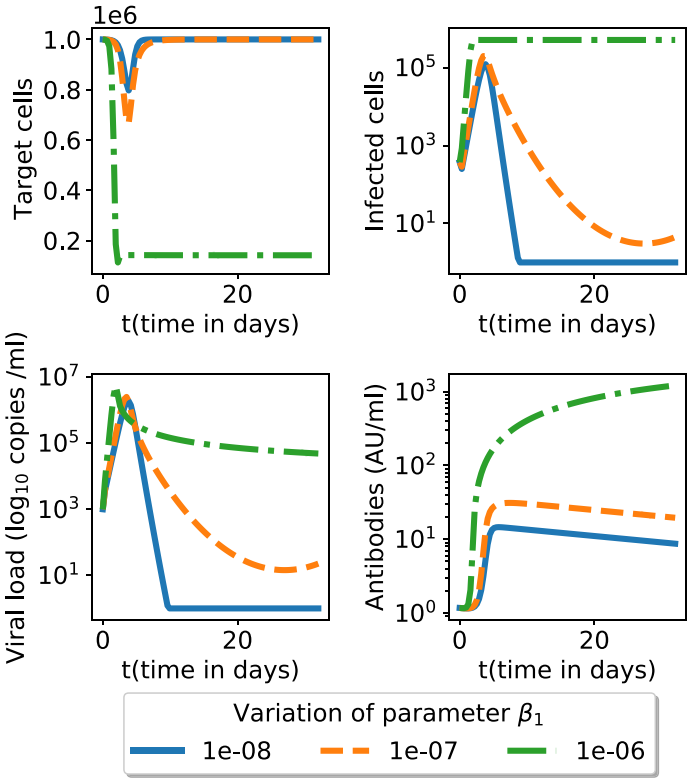

Fig. 5 The effect of the ADE parameter β_1 [the model (1)–(4)]. The secondary (challenge) infection has fixed neutralizing antibodies capacity b but several possible β_1 (ADE) parameter values; for all other parameters we use the nominal values given in Table 1. See Fig. 7 for simulation over a longer time span

5 Discussion

We studied the immune response to infection and reinfection with SARS-CoV-2 using a numerical model; the model can also take into account the possible presence of ADE, either during the first infection or during a challenge (secondary infection or reinfection with a different phenotype, after vaccination, etc.).

As there is no clear evidence to date that ADE occurs in severe COVID-19 patients, we assume that ADE only occurs in the case of challenge.

We started from a classical virus-host dynamic (Wodarz 2007; Tang et al. 2020) and modified it by adding the parameter β_1 to account for a possible ADE mechanism. In order to keep the model at its lowest complexity, we do not distinguish between ADE triggering and neutralising antibodies.

We performed a theoretical study of our system by calculating steady states and stability with and without ADE. We showed that stochastic events can also play a role and prevent the stable steady state from being reached in practice; we identified the parameters b (neutralising capacity) and β_1 (presence of ADE) as crucial for the dynamics of our system.

Next, we calibrated our parameter values to match the reference viral load from the literature (Lescure et al. 2020; Seow et al. 2020) and obtained good results.

We then studied a secondary infection (or an infection following vaccination or another immune event) which may have different immunodynamic parameters. We saw that without ADE, the low neutralising capacity of antibodies was systematically compensated by higher concentrations of antibodies leading to viral clearance. On the other hand, the addition of an ADE was not always associated with viral clearance but possibly with high target cell killing. Simulations and equilibrium analysis showed that the antibody concentration had an upper limit that prevented a higher ADE from being compensated by an unlimited amount of antibody. Therefore, ADE should be taken into consideration as a serious risk in understanding the disease, treatment and vaccine development and programming.

On the other hand, we have shown that the results are sensitive to the capacity of neutralizing antibodies (the b parameter); it should be noted that a decrease in this parameter can occur in several situations, e.g. due to degradation of the immune function, malfunctioning of the antibody immunodominance mechanism that ends up selecting too many weakly neutralizing antibodies or due to poorly calibrated therapeutic interventions. Regardless of the cause, such a decrease in neutralizing capacity is likely to imply a substantial deterioration of the outcome.

In summary, our results seem to confirm that the presence of ADE correlates mainly with significant target cell destruction, whereas the loss of neutralizing capacity correlates with both a higher number of antibodies (leading to inflammation) and a higher target cell destruction.

5.1 Limitations and Future Work

Like any other model, our model of course has several limitations. First, we assumed that all infected cells supported viral replication, including ADE-infected cells. Concerning SARS-CoV-2, the questions of ADE is still under debate, but for SARS-CoV-1 in vitro ADE evidence suggested abortive viral replication in ADE infected cells. Therefore, if we changed the model (1)–(4) to include this distinction, the steady state would change and ADE could be compensated for. Similarly, we did not distinguish between old and new antibodies secreted upon challenge. This would involve more parameters and change the equilibrium levels but not intrinsically change the behavior of the variables. The dynamic antibody model can also be modified to include, for example, constant antibody production after a threshold or more specific effects (André et al. 2006; Pawelek et al. 2016). As far as parameter are concerned, we did not have enough usable data to train our model and better fit the parameters. Finally, a single model can hardly account for the extreme variability in clinical outcomes of COVID-19, see Callaway et al. (2020); some studies proposed that part of this variability comes from genetics, see e.g., Ellinghaus et al. (2020) where genetic information from about 4,000 people from Italy and Spain was correlated with COVID-19 severity. This may lead to a variability of our model parameters in the form of random variables.

To date (January 2022), billions of people have been vaccinated, at least by one injection, and over half a billion have been infected. Fortunately, despite the spread of the highly contagious omicron variant, it appears that morbidity and mortality are declining. This implies that, for the time being, the most disastrous consequences of the phenomena included in this model are not being observed. However, it must be emphasized that human polymorphism, viral polymorphism and highly variable environmental conditions, as well as the considerable variety of vaccination protocols, mean that there may be isolates where ADE or the other immune responses we have explored could be significant. It is therefore particularly important to monitor variations in morbidity and mortality around the world so that a rapid response can be implemented if there is a local increase. Finally, the types of vaccines used are very different. For those based on well-established technologies, we do not foresee any consequences other than those discussed in this work, except perhaps in terms of vaccination protocols (time between primary and booster injections. In contrast, the use of vaccines based on indirect antigen production (adenovirus or synthetic RNA-based vaccines) requires specific encapsulation of the active ingredient in a variety of capsules or cassettes. These containers can, by themselves, be immunogenic. The consequence would be that after several immunisations, patients would develop a response against the vaccine, rendering it ineffective against the disease. We have not considered this possibility in our work.

Another limitation of this work is that in a secondary challenge there would be presumably already present memory cells allowing for a faster antibody response, thus increasing the value of $A(0)$ relatively to a primary infection. This circumstance was not considered in this work.

The more science sheds light on the full picture of SARS-CoV-2, the more complex and precise details our model can go into. In the meantime, the main take-home message is that, with parameters consistent with the available clinical data, neutralizing capacity and ADE mechanisms can play an important immunological role in the outcome of primary and secondary infection.

Appendix 1: Choice of Simulation Parameters

Parameters' order of magnitude were derived from literature, see Lee et al. (2009) for μ, Lescure et al. (2020) for ω, clearance data from Tang et al. (2020), Li et al. (2020), Long et al. (2020) and Seow et al. (2020). To obtain the precise values, we then fitted the model to the SARS-CoV-2 clinical data available in Fig. 2 and obtained the values in Table 1 (simulation results are shown in Fig. 3).

Appendix 2: Sensitivity with Respect to Parameters

We plot here a longer time evolution corresponding to Figs. 4 and 5. This allows to see the difference between initial dynamics and the long time equilibrium, cf. considerations in Sect. 3.3.

Appendix 3: Mathematical Properties of the Model

We describe in an incremental way the mathematical properties of the main model (1)–(5). We take advantage of this description to illustrate the hypotheses (6) and (7). The results in "Model Without a Virus, Nor Immune Response" section and "Model: Virus and Immune Response but No Enhancement" section in "Appendix 3" are known, see e.g., Perelson et al. (1993), Nowak and May (2000), Smith et al. (2003) and Wodarz (2007) while those in the main text (Propositions 1, 2 and their proofs in this appendix) are, to the best of our knowledge, original.

Model Without a Virus, Nor Immune Response

In absence of any infection the equations for the target cells are (see Wodarz 2007; Nowak and May 2000):

$$dT/dt = \Lambda - \mu T. \tag{16}$$

Since the Jacobian matrix at equilibrium (a 1×1 matrix) is the constant $-\mu$ therefore the equilibrium is stable, in fact any initial data $T(0)$ will converge to the equilibrium

$$T^* = \Lambda/\mu. \tag{17}$$

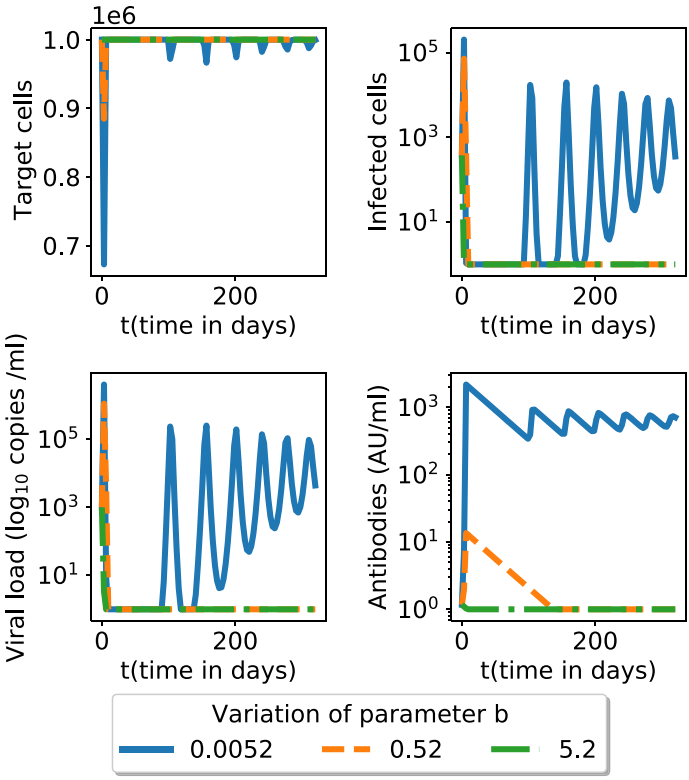

Fig. 6 Simulation in Fig. 4 for a longer time span

Model with Virus but No Immune Response

We employ the basic model of virus dynamics, see Nowak and May (2000, Eq. (3.1), p. 18) and also Wodarz (2007, Eqs. (2.3)–(2.4), p. 26) described by the equations:

$$dT/dt = \Lambda - \mu T - \beta_0 VT, \tag{18}$$

$$dI/dt = \beta_0 VT - \delta I, \tag{19}$$

$$dV/dt = \omega I - cV. \tag{20}$$

The initial conditions are:

$$T(0) = T^* = \Lambda/\mu,\ I(0) = 0,\ V(0) > 0, \tag{21}$$

which express the fact that the initial state for T is the stable equilibrium seen in "Model Without a Virus, Nor Immune Response" section in "Appendix 3", there are initially no infected cells and the initial viral load is strictly positive.

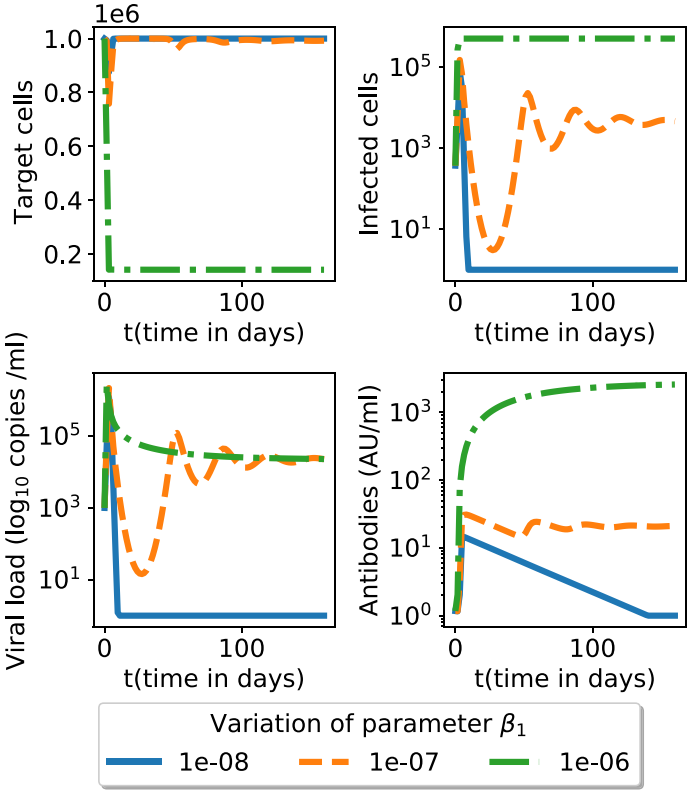

Fig. 7 Simulation in 5 for a longer time span

It is natural to assume that the decay rate of infected cells is at least as large as the decay rate of healthy cells, i.e., assumption (6).

In this model, an infection is only possible if the basic reproduction ratio of the virus in the absence of immune response, defined in (8) is strictly super-unitary, that is

$$R_0 > 1. \tag{22}$$

Otherwise, that is if $R_0 \leq 1$, the initial viral load can only decrease. The model has two equilibria:

- trivial equilibrium: $T = T^* = \Lambda/\mu$, $V = I = 0$. The Jacobian matrix at equilibrium is $\begin{pmatrix} -\mu & 0 & -\beta_0 T^* \\ 0 & -\delta & \beta_0 T^* \\ 0 & \omega & -c \end{pmatrix}$. The eigenvalues of this matrix, under condition (22), are all real but not all negative: one of them is $\lambda_1 = -\mu$ but the product of the other two is $\delta c - \omega\beta_0 T^* \leq 0$ thus at least one is positive. Therefore, under assumption (22), this critical point is not a stable equilibrium.

- the "immunosuppression" equilibrium (11)

The Jacobian matrix is $J = \begin{pmatrix} -\mu - \beta_0 V^{is} & 0 & -\beta_0 T^{is} \\ \beta_0 V^{is} & -\delta & \beta_0 T^{is} \\ 0 & \omega & -c \end{pmatrix}$; the characteristic polynomial $P(X) = det(X \cdot I - J)$ can be computed directly and is $P(X) = (X+\delta)(X+c)(X+\mu+\beta_0 V^{is}) - \delta c(X+\mu)$. Denote λ_i, $i = 1,2,3$ the roots of $P(X)$. Note that $P(-\delta - c - \mu - \beta_0 V^{is}) = -(c+\mu+\beta_0 V^{is})(\delta+\mu+\beta_0 V^{is})(\delta+c) + \delta c(\delta+c+\beta_0 V^{is}) < 0$ (only negative factors remain after immediate simplifications) and $P(0) = \delta c \beta_0 V^{is} > 0$. Thus $P(X)$ has a negative real root, denote it λ_1, such that $-\delta - c - \mu - \beta_0 V^{is} < \lambda_1 < 0$. The product of all roots is $-P(0) = -\delta c \beta_0 V^{is} < 0$, thus $\lambda_2 \cdot \lambda_3 > 0$; the sum of all roots is $-\delta - c - \mu - \beta_0 V^{is} < \lambda_1$, which means that $\lambda_2 + \lambda_3 < 0$. It follows that both λ_2 and λ_3 have negative real part. Therefore the equilibrium is stable.

Note that this conclusion can also be reached using the Routh–Hurwitz criterion (see an example of use below).

It is important to note that the viral load V^{is} is the viral load that the infection will cause in a completely immunodeficient individual. We expect V^{is} to be significantly high, see in "Model: Virus and Immune Response but No Enhancement" section in "Appendix 3" for details.

Model: Virus and Immune Response but No Enhancement

In this section we consider the model (1)–(4) with no ADE i.e., $\beta(A) = \beta_0$ that is $\beta_1 = 0$. This model is similar to other in the literature (see for instance Wodarz 2007, eq. (2.9), p. 29) who consider also the cytotoxic effect of the immune response on the infected cells; however they do not consider virus destruction by antibodies. In particular there virus load is constant. Another similar model is Wodarz (2007), Eqs. (8.1)–(8.3). With respect to the previous section here the immune response is present. It is triggered by a threshold set at V^t (see definition in (9)). It is natural to suppose that the immune response threshold is a very small value and in any case a value smaller than the immunosupression viral load V^{is} in (11). That is we can make the hypothesis that $V^{is} > V^t$ i.e. assumption (7) holds.

The Jacobian matrix is:

$$J = \begin{pmatrix} -(\mu + \beta_0 V^{is}) & 0 & -\beta_0 T & 0 \\ \beta_0 V & -\delta & \beta_0 T & 0 \\ 0 & \omega & -(c+bA) & -bV \\ 0 & 0 & aA & aV - \sigma \end{pmatrix}. \tag{23}$$

With these provisions, one can find analytically the critical points (equilibria candidates):

1. $T = T^* = \Lambda/\mu, V = I = A = 0$, which is the high dimensional analog of equilibrium (17). However, unlike in "Model Without a Virus, Nor Immune Response"

section in Appendix 3, this equilibrium is not stable any more (the determinant of the Jacobian matrix is negative when hypothesis (22) is satisfied.

2. the immunosuppression equilibrium (11) with $A = 0$; again this equilibrium is not stable any more because the condition (7) implies that the eigenvalue $aV^{is} - \sigma$ is positive.
3. the only critical point left is (10). We prove that it is stable in the following. Note that the equilibrium value of the antibody level is positive due to condition (7).

Proof of the Proposition 1 The equilibrium is stable when the real parts of the eigenvalues of the Jacobian matrix are negative. This is the same as saying that the roots of the polynomials $P_0(X) = det(X \cdot I - J)$ have negative real parts (here I is the identity matrix). Such a polynomial is called stable and, if we write $P_0(X) = \gamma_4 X^4 + \gamma_3 X^3 + \gamma_2 X^2 + \gamma_1 X^1 + \gamma_0$ then, following the Routh–Hurwitz criterion Routh (1877), (Gradshteyn and Ryzhik 2000, p. 1076), the stability holds true when

$$\gamma_k > 0, k = 0, 1, 2, 3, 4 \tag{24}$$

and

$$\gamma_1\gamma_2\gamma_3 > \gamma_4\gamma_1^2 + \gamma_3^2\gamma_0. \tag{25}$$

Unfortunately, checking in general these conditions is very difficult because the expressions involved are highly non-linear in the original parameters of the model (a,b, c, σ, etc.). We therefore need to exploit to the full extent the specific setting of our model. To this end we will make the following change of variables:

$$\zeta = \delta - \mu > 0, \quad w = R_0 - 1 - \frac{\sigma\beta_0}{\mu a} > 0. \tag{26}$$

After replacing all new variables and direct computations, we obtain:

$$\gamma_0 = c\delta\mu\sigma w, \gamma_1 = \frac{c\sigma\left(a^2\delta\mu w + a^2\mu^2 w + a\beta_0\delta\mu w + a\beta_0\delta\mu + a\beta_0\mu\sigma w + \beta_0^2\delta\sigma\right)}{a\left(a\mu + \beta_0\sigma\right)},$$
$$\gamma_2 = \frac{a^2c\mu^2 w + a^2c\mu^2 + a^2c\mu\sigma w + a^2\delta\mu^2 + a\beta_0 c\mu\sigma w + 2a\beta_0 c\mu\sigma + 2a\beta_0\delta\mu\sigma + \beta_0^2 c\sigma^2 + \beta_0^2\delta\sigma^2}{a\left(a\mu + \beta_0\sigma\right)},$$
$$\gamma_3 = \frac{a^2\delta\mu + a^2\mu^2 + a\beta_0\delta\sigma + 2a\beta_0\mu\sigma + ac\left(a\mu(w+1) + \beta_0\sigma\right) + \beta_0^2\sigma^2}{a\left(a\mu + \beta_0\sigma\right)}, \gamma_4 = 1.$$

Since all parameters involved are positive we obtain that the condition (24) is satisfied. To check the remaining condition (25) we obtain

$$\gamma_1\gamma_2\gamma_3 - \gamma_4\gamma_1^2 + \gamma_3^2\gamma_0 = \frac{ac}{a^3\left(a\mu + \beta_0\sigma\right)^3} Q_0(w, a, c, \beta_0, \mu, \sigma, \zeta), \tag{27}$$

where the multi-variable polynomial Q_0 is seen, after long but straightforward computations (see also the symbolic computation code Danchin et al. (2020)) to be equal to :

$$
\begin{aligned}
Q_0(w,a,c,\beta_0,\mu,\sigma,\zeta) = {} & w^3a^6c^2\mu^5 + 2w^3a^6c^2\mu^4\sigma + w^3a^6c^2\mu^3\sigma\zeta + w^3a^5c^2\beta_0\mu^5 \\
& + 3w^3a^5c^2\beta_0\mu^4\sigma + w^3a^5c^2\beta_0\mu^4\zeta + w^3a^5c^2\beta_0\mu^3\sigma^2 \\
& + w^3a^5c^2\beta_0\mu^3\sigma\zeta + w^3a^4c^2\beta_0^2\mu^4\sigma + w^3a^4c^2\beta_0^2\mu^3\sigma^2 + w^3a^4c^2\beta_0^2\mu^3\sigma\zeta \\
& + 2w^2a^6c^2\mu^5 + 2w^2a^6c^2\mu^4\sigma + w^2a^6c^2\mu^3\sigma\zeta + 2w^2a^6c\mu^6 \\
& + w^2a^6c\mu^5\zeta + 3w^2a^5c^2\beta_0\mu^5 + 8w^2a^5c^2\beta_0\mu^4\sigma + 3w^2a^5c^2\beta_0\mu^4\zeta \\
& + 3w^2a^5c^2\beta_0\mu^3\sigma^2 + 2w^2a^5c^2\beta_0\mu^3\sigma\zeta + w^2a^5c^2\beta_0\mu^2\sigma^2\zeta + 3w^2a^5c\beta_0\mu^6 \\
& + 5w^2a^5c\beta_0\mu^5\sigma + 5w^2a^5c\beta_0\mu^5\zeta + 2w^2a^5c\beta_0\mu^4\zeta^2 - w^2a^5c\beta_0\mu^3\sigma\zeta^2 \\
& + 6w^2a^4c^2\beta_0^2\mu^4\sigma + 8w^2a^4c^2\beta_0^2\mu^3\sigma^2 + 6w^2a^4c^2\beta_0^2\mu^3\sigma\zeta + w^2a^4c^2\beta_0^2\mu^2\sigma^3 \\
& + 2w^2a^4c^2\beta_0^2\mu^2\sigma^2\zeta + 6w^2a^4c\beta_0^2\mu^5\sigma + 6w^2a^4c\beta_0^2\mu^4\sigma^2 + 9w^2a^4c\beta_0^2\mu^4\sigma\zeta \\
& - w^2a^4c\beta_0^2\mu^3\sigma^2\zeta + 3w^2a^4c\beta_0^2\mu^3\sigma\zeta^2 - w^2a^4c\beta_0^2\mu^2\sigma^2\zeta^2 + 3w^2a^3c^2\beta_0^3\mu^3\sigma^2 \\
& + 2w^2a^3c^2\beta_0^3\mu^2\sigma^3 + 3w^2a^3c^2\beta_0^3\mu^2\sigma^2\zeta + 4w^2a^3c\beta_0^3\mu^4\sigma^2 + 4w^2a^3c\beta_0^3\mu^3\sigma^3 \\
& + 5w^2a^3c\beta_0^3\mu^3\sigma^2\zeta + w^2a^3c\beta_0^3\mu^2\sigma^2\zeta^2 + w^2a^2c\beta_0^4\mu^3\sigma^3 + w^2a^2c\beta_0^4\mu^2\sigma^4 \\
& + w^2a^2c\beta_0^4\mu^2\sigma^3\zeta + wa^6c^2\mu^5 + 2wa^6c\mu^6 + wa^6c\mu^5\zeta + 3wa^5c^2\beta_0\mu^5 \\
& + 5wa^5c^2\beta_0\mu^4\sigma + 3wa^5c^2\beta_0\mu^4\zeta + wa^5c^2\beta_0\mu^3\sigma\zeta + 6wa^5c\beta_0\mu^6 \\
& + 7wa^5c\beta_0\mu^5\sigma + 10wa^5c\beta_0\mu^5\zeta + wa^5c\beta_0\mu^4\sigma\zeta + 4wa^5c\beta_0\mu^4\zeta^2 \\
& - wa^5c\beta_0\mu^3\sigma\zeta^2 + 2wa^5\beta_0\mu^7 + 5wa^5\beta_0\mu^6\zeta + 4wa^5\beta_0\mu^5\zeta^2 \\
& + wa^5\beta_0\mu^4\zeta^3 + 9wa^4c^2\beta_0^2\mu^4\sigma + 8wa^4c^2\beta_0^2\mu^3\sigma^2 + 9wa^4c^2\beta_0^2\mu^3\sigma\zeta \\
& + 2wa^4c^2\beta_0^2\mu^2\sigma^2\zeta + 18wa^4c\beta_0^2\mu^5\sigma + 11wa^4c\beta_0^2\mu^4\sigma^2 + 28wa^4c\beta_0^2\mu^4\sigma\zeta \\
& - wa^4c\beta_0^2\mu^3\sigma^2\zeta + 10wa^4c\beta_0^2\mu^3\sigma\zeta^2 - 2wa^4c\beta_0^2\mu^2\sigma^2\zeta^2 + 7wa^4\beta_0^2\mu^6\sigma \\
& + 17wa^4\beta_0^2\mu^5\sigma\zeta + 13wa^4\beta_0^2\mu^4\sigma\zeta^2 + 3wa^4\beta_0^2\mu^3\sigma\zeta^3 + 9wa^3c^2\beta_0^3\mu^3\sigma^2 \\
& + 5wa^3c^2\beta_0^3\mu^2\sigma^3 + 9wa^3c^2\beta_0^3\mu^2\sigma^2\zeta + wa^3c^2\beta_0^3\mu\sigma^3\zeta + 20wa^3c\beta_0^3\mu^4\sigma^2 \\
& + 10wa^3c\beta_0^3\mu^3\sigma^3 + 28wa^3c\beta_0^3\mu^3\sigma^2\zeta - wa^3c\beta_0^3\mu^2\sigma^3\zeta + 8wa^3c\beta_0^3\mu^2\sigma^2\zeta^2 \\
& - wa^3c\beta_0^3\mu\sigma^3\zeta^2 + 9wa^3\beta_0^3\mu^5\sigma^2 + 21wa^3\beta_0^3\mu^4\sigma^2\zeta + 15wa^3\beta_0^3\mu^3\sigma^2\zeta^2 \\
& + 3wa^3\beta_0^3\mu^2\sigma^2\zeta^3 + 3wa^2c^2\beta_0^4\mu^2\sigma^3 + wa^2c^2\beta_0^4\mu\sigma^4 + 3wa^2c^2\beta_0^4\mu\sigma^3\zeta \\
& + 10wa^2c\beta_0^4\mu^3\sigma^3 + 5wa^2c\beta_0^4\mu^2\sigma^4 + 12wa^2c\beta_0^4\mu^2\sigma^3\zeta + 2wa^2c\beta_0^4\mu\sigma^3\zeta^2 \\
& + 5wa^2\beta_0^4\mu^4\sigma^3 + 11wa^2\beta_0^4\mu^3\sigma^3\zeta + 7wa^2\beta_0^4\mu^2\sigma^3\zeta^2 + wa^2\beta_0^4\mu\sigma^3\zeta^3 \\
& + 2wac\beta_0^5\mu^2\sigma^4 + wac\beta_0^5\mu\sigma^5 + 2wac\beta_0^5\mu\sigma^4\zeta + wa\beta_0^5\mu^3\sigma^4 \\
& + 2wa\beta_0^5\mu^2\sigma^4\zeta + wa\beta_0^5\mu\sigma^4\zeta^2 + a^5c^2\beta_0\mu^5 + a^5c^2\beta_0\mu^4\zeta + 3a^5c\beta_0\mu^6 \\
& + 5a^5c\beta_0\mu^5\zeta + 2a^5c\beta_0\mu^4\zeta^2 + 2a^5\beta_0\mu^7 + 5a^5\beta_0\mu^6\zeta + 4a^5\beta_0\mu^5\zeta^2 \\
& + a^5\beta_0\mu^4\zeta^3 + 4a^4c^2\beta_0^2\mu^4\sigma + 4a^4c^2\beta_0^2\mu^3\sigma\zeta + 12a^4c\beta_0^2\mu^5\sigma + 19a^4c\beta_0^2\mu^4\sigma\zeta \\
& + 7a^4c\beta_0^2\mu^3\sigma\zeta^2 + 9a^4\beta_0^2\mu^6\sigma + 22a^4\beta_0^2\mu^5\sigma\zeta + 17a^4\beta_0^2\mu^4\sigma\zeta^2 + 4a^4\beta_0^2\mu^3\sigma\zeta^3 \\
& + 6a^3c^2\beta_0^3\mu^3\sigma^2 + 6a^3c^2\beta_0^3\mu^2\sigma^2\zeta + 19a^3c\beta_0^3\mu^4\sigma^2 + 28a^3c\beta_0^3\mu^3\sigma^2\zeta + 9a^3c\beta_0^3\mu^2\sigma^2\zeta^2 + 16a^3\beta_0^3\mu^5\sigma^2 \\
& + 38a^3\beta_0^3\mu^4\sigma^2\zeta + 28a^3\beta_0^3\mu^3\sigma^2\zeta^2 + 6a^3\beta_0^3\mu^2\sigma^2\zeta^3 + 4a^2c^2\beta_0^4\mu^2\sigma^3 \\
& + 4a^2c^2\beta_0^4\mu\sigma^3\zeta + 15a^2c\beta_0^4\mu^3\sigma^3 + 20a^2c\beta_0^4\mu^2\sigma^3\zeta + 5a^2c\beta_0^4\mu\sigma^3\zeta^2 + 14a^2\beta_0^4\mu^4\sigma^3 + 32a^2\beta_0^4\mu^3\sigma^3\zeta \\
& + 22a^2\beta_0^4\mu^2\sigma^3\zeta^2 + 4a^2\beta_0^4\mu\sigma^3\zeta^3 + ac^2\beta_0^5\mu\sigma^4 + ac^2\beta_0^5\sigma^4\zeta + 6ac\beta_0^5\mu^2\sigma^4 + 7ac\beta_0^5\mu\sigma^4\zeta + ac\beta_0^5\sigma^4\zeta^2 \\
& + 6a\beta_0^5\mu^3\sigma^4 + 13a\beta_0^5\mu^2\sigma^4\zeta + 8a\beta_0^5\mu\sigma^4\zeta^2 + a\beta_0^5\sigma^4\zeta^3 + c\beta_0^6\mu\sigma^5 + c\beta_0^6\sigma^5\zeta + \beta_0^6\mu^2\sigma^5 \\
& + 2\beta_0^6\mu\sigma^5\zeta + \beta_0^6\sigma^5\zeta^2.
\end{aligned}
$$

Most of the monomials in Q_0 have positive coefficients, except the following ones: $-w^2a^5c\beta_0\mu^3\sigma\zeta^2$, $-w^2a^4c\beta_0^2\mu^3\sigma^2\zeta$, $-w^2a^4c\beta_0^2\mu^2\sigma^2\zeta^2$, $-wa^5c\beta_0\mu^3\sigma\zeta^2$, $-wa^4c\beta_0^2\mu^3\sigma^2\zeta$, $-2wa^4c\beta_0^2\mu^2\sigma^2\zeta^2$, $-wa^3c\beta_0^3\mu^2\sigma^3\zeta$, $-wa^3c\beta_0^3\mu\sigma^3\zeta^2$. However, in all cases we can come up with two terms that render the total sum positive. For instance the term $-w^2a^5c\beta_0\mu^3\sigma\zeta^2$ (term 27 of the polynomial) is negative but, when we combine it with the terms $w^3a^6c^2\mu^3\sigma\zeta/2$ (half of thethird term) and $wa^4\beta_0^2\mu^3\sigma\zeta/2$ (half of the term 79), both appearing with positive coeffcients, we obtain a positive number $w^3a^6c^2\mu^3\sigma\zeta/2 - w^2a^5c\beta_0\mu^3\sigma\zeta^2 + wa^4\beta_0^2\mu^3\sigma\zeta^3/2 = \frac{wa\mu^3\sigma\zeta}{2}(wac - \beta_0\zeta)^2 \geq 0$.

The interested reader can check that in the same way that:

- the 36th monomial compensate with monomials 7 and 92;
- the 38th monomial compensate with monomials 3 and 104;
- the 61th monomial compensate with monomials 14 and 128;
- the 73th monomial compensate with monomials 13 and 145;
- the 75th monomial compensate with monomials 14 and 146;
- the 87th monomial compensate with monomials 20 and 154;
- the 89th monomial compensate with monomials 22 and 155.

This allows to state that $Q_0 > 0$ which concludes the proof. which concludes the proof. □

Full Model: Virus, Immune System and ADE

Proof of the Proposition 2 We consider the model (1)–(4) with $\beta(A) = \beta_0 + \beta_1 A$ ($\beta_1 > 0$). The analysis of this dynamics is more involved. The first two equilibria, having $A = 0$ are the complete analogues of the equilibria seen in previous sections and have no dynamical interest. Since $A = 0$ the parameter β_1 that multiplies A has no impact and the proof of the instability of the trivial equilibrium and immunosupression equilibrium follow exactly the same arguments as before.

To find the third equilibrium, note that after immediate computations we find that the antibody level is solution of the second order equation (12). Such an equation has two solutions but exactly one is positive because the product of roots is negative; thus only a single point is an admissible equilibrium, namely the positive solution of (12) (with respect to the unknown A); setting to zero all derivatives we obtain the other values as in (13).

To prove the properties of this equilibrium we start with the point 3c of the proposition; consider the values $a = \sigma = c = b = \omega = 1, \mu = 1.e{-}3, \delta = 2, \Lambda = 4, \beta_0 = 0.0011$ and $\beta_1 = 0.01188$; all hypotheses are satisfied and the numerical values of the equilibrium are $T = 333.33, I = 1.83, V = 1, A = 0.83$ while the eigenvalues are -3.45, 0.50, 0.01 and -0.90. Since some eigenvalues are real and positive the equilibrium is not stable for this set of parameters. This completes the proof for this point. In practice the

evolution oscillates indefinitely between a state with high T value and one with very low T value.

Note that the point 3a of the conclusion is just a consequence of the continuity and the proposition 1, because both the equilibrium and the coefficients of the polynomial $P(X) = \det(X \cdot I - J)$ evaluated at the equilibrium depend smoothly on β_1. Since we proved that (24) and (25) are true for $\beta_1 = 0$ by continuity the terms in the two conditions will remain strictly positive for β_1 small enough and by the Routh–Hurwitz criterion the equilibrium will be stable.

The only point remaining to be proved is 3b. Note that when $\beta_1 \to \infty$ the positive root A^f of the Eq. (12) converges to some quantity A^∞, and $\beta(A^f) \to \infty$; moreover, we obtain from the definition of T^f that $\lim_{\beta_1 \to \infty} T^f = 0$ and $\lim_{\beta_1 \to \infty}(\beta(A^f)T^f) = \lim_{\beta_1 \to \infty}(\beta_1 T^f) = \frac{\delta(c+bA^\infty)}{\omega A^\infty}$. Consider the Jacobian matrix:

$$J = \begin{pmatrix} -\beta(A)V - \mu & 0 & -\beta(A)T & -\beta_1 TV \\ \beta(A)V & \delta & \beta(A)T & \beta_1 TV \\ 0 & \omega & -(c+bA) & -bV \\ 0 & 0 & aA & aV - \sigma \end{pmatrix}. \tag{28}$$

Let us compute $P(X) = \det(X \cdot I - J) = \det(J - X \cdot I)$:

$$\begin{aligned} P(X) &= \begin{vmatrix} -\beta(A)V - \mu - X & 0 & -\beta(A)T & -\beta_1 TV \\ \beta(A)V & -\delta - X & \beta(A)T & \beta_1 TV \\ 0 & \omega & -X - (c+bA) & -bV \\ 0 & 0 & aA & -X \end{vmatrix} \\ &= \begin{vmatrix} -\mu - X & -\delta - X & 0 & 0 \\ \beta(A)V & -\delta - X & \beta(A)T & \beta_1 TV \\ 0 & \omega & -X - (c+bA) & -bV \\ 0 & 0 & aA & -X \end{vmatrix} \\ &= -(\mu + X)\begin{vmatrix} -\delta - X & \beta(A)T & \beta_1 TV \\ \omega & -X - (c+bA) & -bV \\ 0 & aA & -X \end{vmatrix} - \beta(A)V \begin{vmatrix} -\delta - X & 0 & 0 \\ \omega & -X - (c+bA) & -bV \\ 0 & aA & -X \end{vmatrix}. \end{aligned}$$

Thus the polynomial $P(X) = \det(X \cdot I - J)$ can be written, to first order in β_1, as $P(X) = R(X) + \beta(A)V(X + \delta)(X^2 + X(c + bA) + aAbV)$, where $R(X)$ is a fourth order polynomial with leading term X^4 and coefficients independent of β_1. Note that $(X + \delta)(X^2 + X(c + bA) + aAbV)$ is a stable polynomial. To finish the proof we invoke Lemma 1 below for $\psi = \beta(A)V$.

□

Lemma 1 *Let $Z_3 = \phi_3 X^3 + \phi_2 X^2 + \phi_1 X + \phi_0$ be a stable polynomial of order 3 with $\phi_3 > 0$ and $Z_4 = \varphi_4 X^4 + \varphi_3 X^3 + \varphi_2 X^2 + \varphi_1 X + \varphi_0$ a polynomial of order four with $\varphi_4 > 0$. Then, for ψ large enough the polynomial $Z_4(X) + \psi Z_3(X)$ is stable.*

Proof Since $\phi_3 > 0$ using the reciprocal of the Routh–Hurwitz criterion all coefficients ϕ_k are strictly positive and $\phi_1\phi_2 > \phi_0\phi_3$. For ψ large enough this allows to check the Routh–Hurwitz criterion for the fourth order polynomial

$Z_4(X) + \psi Z_3(X)$: the coefficients will be positive and the last remaining condition is $(\varphi_1 + \psi\phi_1)(\varphi_2 + \psi\phi_2)(\varphi_3 + \psi\phi_3) > (\varphi_0 + \psi\phi_0)(\varphi_3 + \psi\phi_3)^2 + (\varphi_1 + \psi\phi_1)\varphi_4^2$, which is satisfied for ψ large enough (leading term $(\phi_1\phi_2 - \phi_0\phi_3)\phi_3$ is positive).

□

Appendix 4: Extended Model Including a Latent Phase

We present here a version of the main model (1)–(5) extended to take into account a latent phase of the cells. The interest of such a model is to give a finer description of all states of the attacked cells; this comes however at the price of requiring several more parameters (including the transition rate $\eta > 0$ from the latent to infected, virus-producing, cells). In practice the choice of the model depends on the outcomes of interest and available data to fit. In our case the data to fit was relatively scarce thus we kept the restricted model (1)–(5) for the numerical simulations. Denoting L the number of latent infected cells (i.e., cells already infected but not yet producing viruses) we can write this model as:

$$dT/dt = \Lambda - \mu T - \beta(A)VT \tag{29}$$

$$dL/dt = \beta(A)VT - \eta L - \mu L \tag{30}$$

$$dI/dt = \eta L - \delta I \tag{31}$$

$$dV/dt = \omega I - cV - bAV \tag{32}$$

$$dA/dt = aVA - \sigma A \tag{33}$$

$$\beta(A) = \beta_0 + \beta_1 A. \tag{34}$$

The model is illustrated in Fig. 8. A rigorous theoretical analysis of this model could be undertaken along the lines presented in the previous sections: because the dI/dt equation is linear in I and L the equilibria will be, up to some constants, very similar; however the stability analysis, still using the Routh–Hurwitz criterion, is more involved and a full analysis is beyond the scope of this paper.

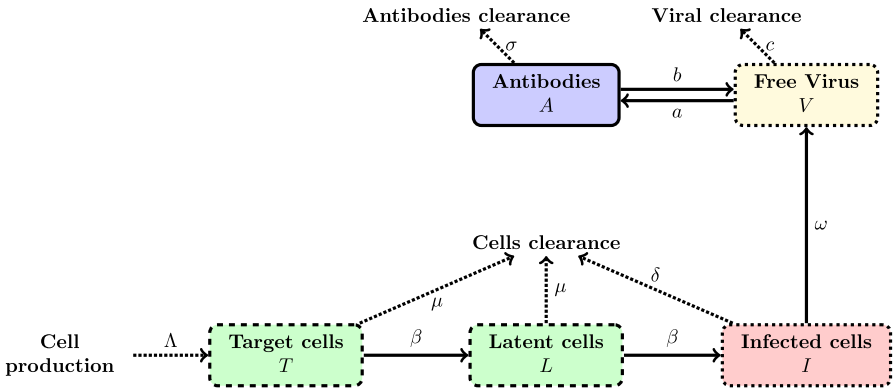

Fig. 8 Graphical illustration of the flow in the model (29)–(34)

Supplementary Information The online version contains supplementary material available at https://doi.org/10.1007/s10441-022-09447-1.

Acknowledgements Ghozlane Yahiaoui is supported by the Engineering and Physical Sciences Research Council (EPSRC): CDT Grant Ref. EP/L015811/1.

References

André J-B, Gandon.S (2006) Vaccination, within–host dynamics and virulence evolution. Evolution 60(1):13–23

Callaway E, Ledford H, Mallapaty S (2020) Six months of coronavirus: the mysteries scientists are still racing to solve. Nature 583(7815):178–179

Castro M, Lythe G, Molina-Paris C, Ribeiro RM (2016) Mathematics in modern immunology. Interface Focus 6(2):20150093

Danchin A, Ng TW, Turinici G (2021) A new transmission route for the propagation of the SARS-CoV-2 coronavirus. Biology 10(1):10

Danchin A, Pagani O, Turinici G, Yahiaoui G (2020) Python symbolic computations for the paper doi 10.1101/2020.10.21.20216713 (Version 1). Zenodo. https://doi.org/10.5281/zenodo.6515163

Danchin A, Pagani O, Turinici G, Yahiaoui G (2020). Supplementary information: Covid-19 adaptive humoral immunity models: weakly neutralizing versus antibody-disease enhancement scenarios. medRxiv. https://doi.org/10.1101/2020.10.21.20216713

Danchin A, Turinici G (2021) Immunity after COVID-19: protection or sensitization? Math Biosci 331:108499

Diekmann O, Heesterbeek JAP (2000) Mathematical epidemiology of infectious diseases: model building, analysis and interpretation, vol 5. Wiley, Hoboken

Dolbeault J, Turinici G (2020) Heterogeneous social interactions and the COVID-19 lockdown outcome in a multi-group SEIR model. Math Model Nat Phenom 15:36

Drożdżal S, Rosik J, Lechowicz K, Machaj F, Szostak B, Przybyciński Jław, Lorzadeh S, Kotfis K, Ghavami S, Łos MJ (2021) An update on drugs with therapeutic potential for SARS-CoV-2 (COVID-19) treatment. Drug Resist Updat 59:100794

Eftimie Raluca, Gillard Joseph J, Cantrell Doreen A (2016) Mathematical models for immunology: current state of the art and future research directions. Bull Math Biol 78(10):2091–2134

Ellinghaus D, Degenhardt F, Bujanda L, Buti M, Albillos A, Invernizzi P, Fernandez J, Prati D, Baselli G, Asselta R, Grimsrud MM, Milani C, Aziz F, Kassens J, May S, Wendorff M , Wienbrandt L, Uellendahl-Werth F, Zheng T, Yi X, de Pablo R, Chercoles AG, Palom A, Garcia-Fernandez A-E, Rodriguez-Frias F, Zanella A, Bandera A, Protti A, Aghemo A, de Nalda AL, Biondi A,

Caballero-Garralda A, Gori A, Tanck A, Latiano A, Fracanzani AL, Peschuck A, Julia A, Pesenti A, Voza A, Jimenez D, Mateos B, Jimenez BN, Quereda C, Angelini C, Cea C, Solier A, Pestana D, Sandoval E, Paraboschi EM, Navas E, Ceriotti F, Martinelli-Boneschi F, Peyvandi F, Blasi F, Tellez L, Blanco-Grau A, Grasselli G, Costantino G, Cardamone G, Foti G, Aneli S, Kurihara H , ElAbd H, My I, Martin J, Erdmann J, Ferrusquia-Acosta J, Garcia-Etxebarria K, Izquierdo-Sanchez L, Bettini LR, Terranova L, Moreira L, Santoro L, Scudeller L, Mesonero F, Roade L, Schaefer M, Carrabba M, Barciela MMR, Basso MEF, Valsecchi MG, Hernandez-Tejero M, Acosta-Herrera M, D'Angio M, Baldini M, Cazzaniga M, Schulzky M, Cecconi M, Wittig M, Ciccarelli M, Rodriguez-Gandia M, Bocciolone M, Miozzo M, Braun N, Martinez N, Palmieri O, Faverio P, Preatoni P, Bonfanti P, Omodei P, Tentorio P, Castro P, Rodrigues PM, Ortiz AB, Roca RF, Gualtierotti R, Nieto R, Badalamenti S, Marsal S, Matullo G, Pelusi S, Monzani V, Wesse T, Pumarola T, Rimoldi V, Bosari S, Albrecht W, Peter W, Gomez MR, D'Amato M, Duga S, Banales JM, Hov JR, Folseraas T, Valenti L, Franke A, Karlsen TH (2020) The ABO blood group locus and a chromosome 3 gene cluster associate with SARS-CoV-2 respiratory failure in an Italian-Spanish genome-wide association analysis. medRxiv. https://doi.org/10.1101/2020.05.31.20114991

Faraz N, Khan Y, Goufo EFD, Anjum A, Anjum A (2020) Dynamic analysis of the mathematical model of COVID-19 with demographic effects. Z Nat C 75(11–12):389–396

Gradshteyn IS, Ryzhik IM (2000) Table of integrals, series, and products (Jeffrey A, Zwillinger D, translation edited and with a preface). Academic Press, San Diego **(in Russian)**

Hethcote HW (2000) The mathematics of infectious diseases. SIAM Rev 42(4):599–653

Iwasaki A, Yang Y (2020) The potential danger of suboptimal antibody responses in COVID-19. Nat Rev Immunol 20(6):339–341

Jaume M, Yip MS, Cheung CY, Leung HL, Li PH, Kien F, Dutry I, Callendret B, Escriou N, Altmeyer R, Nal B, Daëron M, Bruzzone R, Peiris JSM (2011) Anti-severe acute respiratory syndrome coronavirus spike antibodies trigger infection of human immune cells via a pH- and cysteine protease-independent FcγR pathway. J Virol 85(20):10582–10597

John's Hopkins University (2022) COVID-19 Map—Johns Hopkins Coronavirus Resource Center. https://coronavirus.jhu.edu/map.html

Kermack WO, McKendrick AG (1927) A contribution to the mathematical theory of epidemics. Proc R Soc Lond Ser A 115:700–721

Lee HY, Topham DJ, Park SY, Hollenbaugh J, Treanor J, Mosmann TR, Jin X, Ward BM, Miao H, Holden-Wiltse J, Perelson AS, Zand M, Wu H (2009) Simulation and prediction of the adaptive immune response to influenza A virus infection. J Virol 83(14):7151–7165

Lescure F-X, Bouadma L, Nguyen D, Parisey M, Wicky P-H, Behillil S, Gaymard A, Bouscambert-Duchamp M, Donati F, Le Hingrat Q, Enouf v, Houhou-Fidouh N, Valette M, Mailles A, Lucet J-C, Mentre F, Duval X, Descamps D, Malvy D, Timsit J-F, Lina B, van-der Werf S, Yazdanpanah Y (2020) Clinical and virological data of the first cases of COVID-19 in Europe: a case series. Lancet Infect Dis 20(6):697–706

Li C, Xu J, Liu J, Zhou Y (2020) The within-host viral kinetics of SARS-CoV-2. Math Biosci Eng 17(4):2853

Liu J, Liao X, Qian S, Yuan J, Wang F, Liu Y, Wang Z, Wang F-S, Liu L, Zhang Z (2020) Community transmission of severe acute respiratory syndrome coronavirus 2, Shenzhen, China, 2020. Emerg Infect Dis J 26(6):1320

Long Q-X, Tang X-J, Shi Q-L, Li Q, Deng H-J, Yuan J, Hu J-L, Xu W, Zhang Y, Lv F-J, Su K, Zhang F, Gong J, Wu B, Liu X-M, Li J-J, Qiu J-F, Chen J, Huang A-L (2020) Clinical and immunological assessment of asymptomatic SARS-CoV-2 infections. Nat Med 26(8):1200–1204

Louzoun Y (2007) The evolution of mathematical immunology. Immunol Rev 216(1):9–20

Ng TW, Turinici G, Danchin A (2003) A double epidemic model for the SARS propagation. BMC Infect Dis 3(1):19

Nowak M, May RM (2000) Virus dynamics: mathematical principles of immunology and virology. Oxford University Press, Oxford

Padoan A, Cosma C, Sciacovelli L, Faggian D, Plebani M (2020) Analytical performances of a chemiluminescence immunoassay for SARS-CoV-2 IgM/IgG and antibody kinetics. Clin Chem Lab Med 58(7):1081–1088

Pawelek KA, Dor D, Salmeron C Jr, Handel A (2016) Within-host models of high and low pathogenic influenza virus infections: the role of macrophages. PLoS ONE 11(2):e0150568

Perelson AS, Kirschner DE, De Boer R (1993) Dynamics of HIV infection of CD4+ T cells. Math Biosci 114(1):81–125

Routh EJ (1877) A treatise on the stability of a given state of motion, particularly steady motion. Being the essay to which the Adams prize was adjudged in 1877, in the University of Cambridge. Macmillan and Company, London

Seow J, Graham C, Merrick B, Acors S, Steel KJA, Hemmings O, O'Bryne A, Kouphou N, Pickering S, Galao R, Betancor G, Wilson HD, Signell AW, Winstone H, Kerridge C, Temperton N, Snell L, Bisnauthsing K, Moore A, Green A, Martinez L, Stokes B, Honey J, Izquierdo-Barras A, Arbane G, Patel A, OConnell L, O Hara G, MacMahon E, Douthwaite S, Nebbia G, Batra R, Martinez-Nunez R, Edgeworth JD, Neil SJD, Malim MH, Doores K (2020) Longitudinal evaluation and decline of antibody responses in SARS-CoV-2 infection. Nat Microbiol. https://doi.org/10.1038/s41564-020-00813-8

Smith HL, De Leenheer P (2003) Virus dynamics: a global analysis. SIAM J Appl Math 63(4):1313–1327

Tang B, Xiao Y, Sander B, Kulkarni MA, RADAM-LAC Research Team, Jianhong W (2020) Modelling the impact of antibody-dependent enhancement on disease severity of Zika virus and dengue virus sequential and co-infection. R Soc Open Sci 7(4):191749

Taylor A, Foo S-S, Bruzzone R, Dinh LV, King NJC, Mahalingam S (2015) Fc receptors in antibody-dependent enhancement of viral infections. Immunol Rev 268(1):340–364

Wodarz D (2007) Killer cell dynamics: mathematical and computational approaches to immunology, vol 32. Springer, New York

Yip MS, Leung NHL, Cheung CY, Li PH, Lee HHY, Daëron M, Peiris JSM, Bruzzone R, Jaume M (2014) Antibody-dependent infection of human macrophages by severe acute respiratory syndrome coronavirus. Virol J 11:82

Zou L, Ruan F, Huang M, Liang L, Huang H, Hong Z, Yu J, Kang M, Song Y, Xia J, Guo Q, Song T, He J, Yen H-L, Peiris M, Wu J (2020) SARS-CoV-2 viral load in upper respiratory specimens of infected patients. New Engl J Med 382(12):1177–1179. https://doi.org/10.1056/NEJMc2001737

Publisher's Note Springer Nature remains neutral with regard to jurisdictional claims in published maps and institutional affiliations.